CPCHFT 9 (3) 337 – 496 (2008) · ISSN 1439-4235 · Vol. 9 · No. 3 · February 22, 2008 D55711

A EUROPEAN JOURNAL

CHEMPHYSCHEM

OF CHEMICAL PHYSICS AND PHYSICAL CHEMISTRY

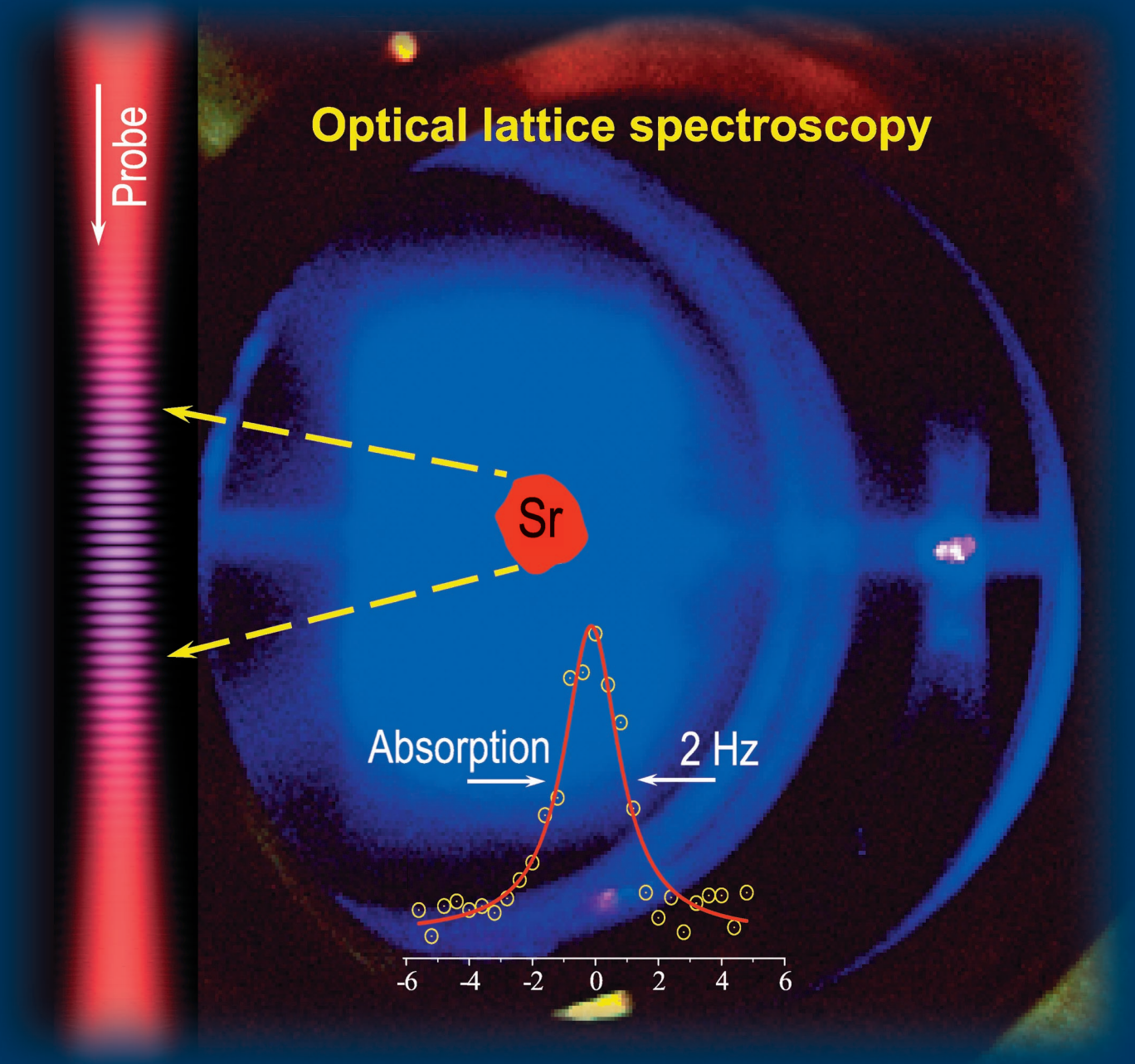

3/2008

Review: Chemistry of Energetically Activated Cumulenes (R. I. Kaiser, A. M. Mebel)
Highlight: Electronic Excited-State Engineering (N. Armaroli)
Concept: Highly Coherent Spectroscopy in Optical Lattices (T. Zelevinsky)

WILEY-VCH

Cover Picture

Tanya Zelevinsky*, Sebastian Blatt, Martin M. Boyd, Gretchen K. Campbell, Andrew D. Ludlow, and Jun Ye

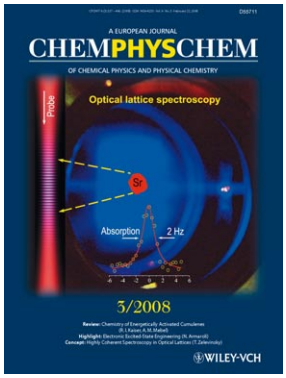

The cover picture shows strontium atoms which are laser cooled to a microkelvin temperature and held in an optical lattice trap. The trap consists of a series of microtraps at the antinodes of the optical standing wave. The intense blue light in the background is the fluorescence of the atoms when they are laser cooled or detected. The clock transition is in red. In their Concept article Zelevinsky et al. (page 375) show that an ultrastable laser recovers a high-resolution spectrum of the narrow, forbidden optical clock transition with a linewidth of 2 Hz. Spectroscopy is performed without recoil shifts, Doppler effects, or ac Stark shifts from the trapping light.

DOI: 10.1002/cphc.200700713

Highly Coherent Spectroscopy of Ultracold Atoms and Molecules in Optical Lattices

Tanya Zelevinsky,* Sebastian Blatt, Martin M. Boyd, Gretchen K. Campbell, Andrew D. Ludlow, and Jun Ye[a]

Cooling and trapping of neutral atoms using laser techniques has enabled extensive progress in precise, coherent spectroscopy. In particular, trapping ultracold atoms in optical lattices in a tight confinement regime allows us to perform high-resolution spectroscopy unaffected by atomic motion. We report on the recent developments of optical lattice atomic clocks that have led to optical spectroscopy coherent at the one second timescale. The lattice clock techniques also open a promising pathway toward trapped ultracold molecules and the possible precision measurement opportunities such molecules offer.

Introduction

Laser cooling and trapping of ensembles of neutral atoms[1] has opened many diverse research fields including experiments with degenerate quantum gases,[2] quantum information,[3] novel precision measurements,[4] optical time and frequency standards,[5–10] and ultracold chemistry.[11]

A large share of the ultracold atom work has been carried out with alkali atoms including Li, Na, K, Rb, and Cs. These atoms have magnetic moments in the ground state that enable magnetic trapping. They also have strongly allowed, laser-accessible electronic transitions from the ground state that facilitate cooling. Magnetic Feshbach resonances allow manipulation of interactions within the cold gas;[12] these resonances take advantage of the non-zero nuclear and electronic spins that give rise to hyperfine level structure in the ground state. However, the hyperfine structure can be a disadvantage for some studies. One example is the comparison of experimental and theoretical properties of cold collisions, where hyperfine structure leads to complicated series of interatomic potentials. Another example is a class of precision measurements that rely on suppressing the effects of external magnetic fields. Besides playing a major role in the studies of ultracold physics, alkali atoms have served as primary and secondary time and frequency standards since the middle of the 20th century. The hyperfine transition in the ground state of ^{133}Cs has been the primary standard since 1967. Although the uncertainty of the Cs clock has now reached only several parts in 10^{16},[13] improvement in its fractional stability, and ultimately the accuracy, is hindered by the relatively small hyperfine transition frequency of 9.2 GHz.

Two-electron atoms such as the alkaline earth metals Mg, Ca, and Sr, as well as isoelectronic Hg and Yb, provide an abundance of bosonic and fermionic isotopes that offer remedies for some of these difficulties. The lack of hyperfine or magnetic structure for the bosonic isotopes with zero nuclear spin results in very simple, theory-friendly interatomic potentials. Most importantly, since the two electron spins can be either antiparallel or parallel, these atoms have spin singlet and triplet energy level manifolds. Since electronic transitions between the two manifolds are spin-forbidden and the ground state is always singlet $^1S_0$, the lowest triplet states tend to be metastable. These metastable states typically lie within an easily laser-accessible range of the ground state, and have very long lifetimes (~10 μs to ~1000 s). The quality factors Q of these ground-metastable transitions, where Q is defined as the ratio of the frequency to the width of the resonance, can reach 10^{18}. Such high-Q transitions are attractive for pushing the precision of ultracold atom experiments to a new regime. The strong cooling transitions of the two-electron atoms are shifted to the blue range of the optical spectrum, where achieving high laser power is more challenging, and the ground states of these atoms have very small magnetic moments, essentially prohibiting magnetic trapping in the ground state. However, with most technical difficulties related to cooling successfully overcome,[14] two-electron atoms offer many benefits to the cold atom research.

In our experiments at JILA, we cool and trap neutral atomic Sr, both the bosonic isotope ^{88}Sr with zero nuclear spin, and the fermionic isotope ^{87}Sr with nuclear spin $I = 9/2$. A spin-forbidden narrow transition allows Sr to be laser cooled below 1 μK, limited by only the recoil momentum of one photon. This low temperature makes Sr a popular choice for labs around the world, pursuing both time standards work and fundamental physics.[6–8, 15]

[a] *Dr. T. Zelevinsky,[+] S. Blatt, Dr. M. M. Boyd, Dr. G. K. Campbell, A. D. Ludlow, Prof. J. Ye*
JILA, National Institute of Standards and Technology and University of Colorado
Boulder, CO 80309-0440 (USA)
Fax: (+1) 303-492-5235
E-mail: tz@phys.columbia.edu

[+] *Current address:*
Department of Physics, Columbia University
538 West 120th Street, New York, NY 10027-5235 (USA)

In order to take advantage of the high-Q electronic transitions, two requirements must be fulfilled. First, the atoms must be held for a sufficiently long time to avoid imposing a Fourier limit on the width of the resonance, and in a way that suppresses motional effects while not causing dephasing of the relevant internal atomic states. These requirements are met by trapping the atoms in a zero-differential-Stark-shift optical lattice in the tight confinement, or Lamb–Dicke, regime. Second, we must have access to an optical probe field that is coherent on the timescale needed to achieve the desired Q. This is provided by a laser stabilized to an ultrahigh finesse passive optical cavity to achieve an optical spectral width below 1 Hz.

Spectroscopy in Optical Lattices

Optical lattices are standing waves of laser light at a wavelength where the trapped atoms have non-zero polarizability. If the wavelength λ is red-detuned from the strongest nearby electronic transition, the atoms are trapped in the strong field regions, or antinodes, of the lattice, with typical spacings of $\lambda/2$. Such a lattice can be 3-dimensional, or 1-dimensional (1D) as is the case here. Only one strong confinement axis exists along which the standing wave is formed, while the remaining dimensions correspond to the width of the focused Gaussian lattice beam (Figure 1). As the atoms move in the planar microscopic traps, they sample the Gaussian intensity profile of the lattice beam, and therefore experience spatially inhomogeneous ac Stark shifts from the trapping field. For atoms in a coherent superposition of the ground and metastable states, the superposition is dephased if the polarizabilities of the two states are significantly different. For this reason, we use an approach sometimes known as the magic wavelength, or zero-differential-Stark-shift, optical lattice.[16,17] We operate the lattice laser at a wavelength of 813 nm where the polarizabilities of the two clock states are equal, such that both states in the superposition see equal trap depths. If the electronic transition is then spectroscopically probed, no net shift or broadening of the resonance profile is observed. This principle is illustrated in Figure 1.

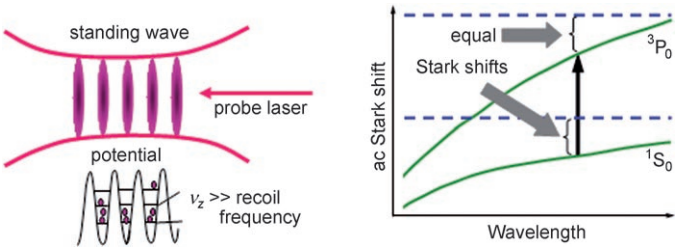

Figure 1. Atoms are trapped at the antinodes of a 1-dimensional optical standing wave (optical lattice). The confinement is tight so that the atomic motion is quantized. In the Lamb–Dicke regime, the trapping frequency ν_z is much larger than the photon recoil frequency associated with an optical probe field. In the resolved sideband regime, this results in spectroscopic features without influences from motional effects such as atom recoil and Doppler broadening. The panel on the right shows that there is no net frequency shift if the lattice wavelength is chosen for matched polarizabilities of the two clock states (not to scale).

Another requirement on the lattice is to preserve the separation of the atomic internal and external degrees of freedom, such that spectroscopy is insensitive to Doppler broadening and photon recoil. The photon recoil $\hbar k$ is the momentum kick transferred to the atom by an absorbed photon with wave vector k, and is mandated by momentum conservation (the recoil energy is $h\varepsilon_r = (\hbar k)^2/(2m)$, where m is the atomic mass and $h = 2\pi\hbar$ is the Planck constant). To decouple these motional effects from electronic level energies, we trap the atoms in the Lamb–Dicke regime.[18] This regime is characterized by a small Lamb–Dicke parameter $\eta = (\varepsilon_r/\nu_z)^{1/2} < 1$, where ν_z is the trap frequency along the strong confinement axis (Figure 1). An alternative way to express the Lamb–Dicke condition in terms of the wavelength of the probe light λ is $\lambda > 2\pi x_0$, where $x_0 = (\hbar/(2\pi m\nu_z))^{1/2}$ is the approximate extent of the atomic wavefunction in the ground state of the lattice trap. Under this condition, the recoil energy is insufficient to excite a motional quantum, so most atoms remain in the original trap state. Although a small fraction of atoms (fraction $\sim\eta^2$) is lost to excited trap states, the majority of atoms are free from any motional energy shifts, including first-order Doppler shifts. The temperature of the sample is now manifested as a distribution among the trap levels. This argument assumes that the spectroscopy probe beam is carefully aligned along the strong confinement axis of the lattice. For our 1D lattice confinement, $\nu_z \cong 50$ kHz and $\varepsilon_r \cong 5$ kHz, so the Lamb–Dicke condition is fulfilled.

In addition to being in the Lamb–Dicke regime, our lattice spectroscopy is typically carried out in the sideband-resolved regime. This means that the observed spectral width (~1 Hz) is much smaller than the axial or radial trap frequencies (50 kHz and 150 Hz, respectively). Under these conditions, insensitivity to transitions that involve a change in the motional state is achieved. When the probe laser frequency is scanned, we observe a carrier transition that corresponds to no net change of the trap state ($\Delta n = 0$), and blue and red sidebands that correspond to $\Delta n = \pm 1$, as shown in Figure 2. The radial sidebands are much closer to the carrier, and are not observed during

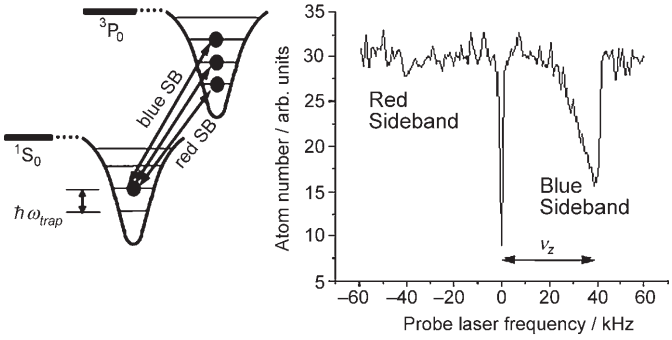

Figure 2. Lattice spectroscopy in the resolved sideband regime. The blue and red sidebands (SB) correspond to the gain and loss of one motional quantum, respectively. The red sideband is suppressed when most atoms are in the ground state of the trap. The central spectral feature has no recoil shift. $^1S_0$ and $^3P_0$ are the clock states.

normal operation owing to the careful alignment of the probe beam. When the probe is tuned to the central carrier, the effect of longitudinal sidebands is doubly suppressed, both by the Lamb–Dicke condition and by frequency detuning.

Optical Lattice Clock

One natural application of the neutral atom system in the Lamb–Dicke resolved-sideband regime is an optical atomic clock with very high stability and accuracy. This approach to atom trapping makes the clock spectroscopy highly insensitive to perturbations as it uses no magnetic fields, and the optical trapping field is carefully engineered to avoid transition shifts. Moreover, the chosen clock states have very small sensitivities to stray magnetic fields.

Neutral Strontium Atomic Clock

The clock transition is the dipole-forbidden $^1S_0$–$^3P_0$ at 698 nm. While strictly forbidden in ^{88}Sr, it is weakly allowed in ^{87}Sr arising from nuclear-spin-induced hyperfine mixing of $^3P_0$ with $^1P_1$ and $^3P_1$. The clock transition has a natural width of ~1 mHz.[16,19,20] Figure 3 shows the relevant Sr energy levels.

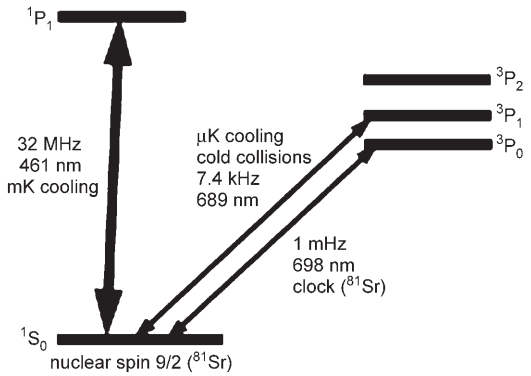

Figure 3. The lowest energy levels of strontium.

The potentially ultrahigh *Q* factor offered by this transition is the main motivation to pursue Sr-based atomic clocks. The smallest possible uncertainty in the knowledge of frequency, or the instability limit of a clock is directly proportional to $1/(QN^{1/2})$, where *N* is the number of atoms contributing to the signal.

The lattice clock apparatus consists of a Zeeman-slowed[21] Sr beam that is loaded into a magneto-optical trap (MOT).[22] The initial MOT operates on the strong $^1S_0$–$^1P_1$ transition at 461 nm with a 32 MHz linewidth (Figure 3). This results in ~10^6 atoms of ^{87}Sr at a millikelvin temperature. The second stage MOT is based on the weak $^1S_0$–$^3P_1$ transition at 689 nm with a 7 kHz linewidth, and yields about 10^5 atoms. When the cooling and trapping lasers and magnetic fields are turned off, about 10^3-10^4 atoms are loaded into the 1D optical lattice. The final atom temperature is between 1–5 μK, depending on the MOT parameters and lattice depth. Since the trap frequency is about 50 kHz, most atoms occupy the ground quantum state of the trap. The longitudinal extent of the atom cloud in the lattice is about 100 lattice sites (~50 μm), and its radius is about 30 μm.

The key component of the optical clock is the local oscillator resonant with the 698 nm $^1S_0$–$^3P_0$ clock transition. This local oscillator is constructed by stabilizing an extended-cavity diode laser[23] to an ultrahigh finesse optical cavity.[24] The initial spectral width of the extended-cavity laser is about 0.5 MHz, and it is narrowed to about a kilohertz by locking to a reflection fringe from an intermediate pre-stabilization cavity. The feedback is applied to the laser diode current and to a piezo-electric transducer (pzt) controlling the length of the laser extended cavity. The narrowed spectrum is then coupled into the final ultrastable cavity with finesse $F \cong 250\,000$, and is further narrowed and stabilized by locking to a reflection fringe. The feedback is applied to an acousto-optical modulator positioned before the ultrahigh finesse cavity and to the pzt that controls the pre-stabilization cavity length. Both cavity locks are based on the Pound–Drever–Hall technique of frequency modulating the laser, and subsequently mixing the modulation frequency source with the optical cavity reflection signal from a photodetector.[25]

The high finesse cavity is placed on a passive vibration-isolation platform and vertically mounted to suppress sensitivity to ground vibrations. The resulting laser spectrum is below ~200 mHz wide as seen on a beat signal with a similar laser for a 5 s integration time (resolution bandwidth limited), and broadens to ~2 Hz in the course of 30 s (limited by nonlinear laser drift because of thermal fluctuations in the cavity mirror substrates and coatings[26]).[24] Figure 4 shows an example of a beat spectrum for ultrastable lasers at two different wavelengths, 698 nm and 1064 nm, taken at the frequency of the 1064 nm laser with the help of a phase-stabilized femtosecond frequency comb.[27]

The clock transition $^1S_0$–$^3P_0$ can be scanned with the 698 nm probe laser, and the absorption lineshape subsequently fitted

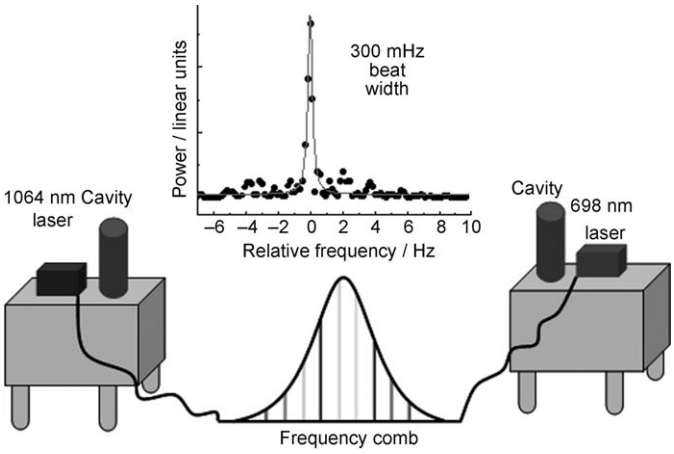

Figure 4. Narrow optical beat between two ultrastable lasers. This trace was obtained with lasers at different wavelengths (698 nm and 1064 nm) that were stabilized to independent high finesse cavities. A femtosecond frequency comb was used to bridge the frequency gap, and the beat was recorded at 1064 nm.

to obtain the line center. With this approach, the clock transition systematic effects have been characterized at the 9×10^{-16} level.[6] In addition, the absolute frequency was determined to 2×10^{-15} (1.1 Hz)[6] by a frequency-comb-based[27] comparison against a hydrogen maser signal calibrated to the NIST-F1 Cs clock.[13] Another mode of clock operation is to stabilize the probe laser on the atomic resonance using slow feedback to steer the laser frequency. This effectively removes the cavity drift of the 698 nm local oscillator, making it suitable for direct comparison with other optical standards. With this second approach, the uncertainty on the systematic effects has reached the 10^{-16} level.[28] Achieving this level of accuracy requires that another optical clock be used as a frequency reference.[10,27,29]

Figure 5 shows a comparison of recent ^{87}Sr clock transition measurements by various labs: JILA,[6,30] Paris,[7] and Tokyo.[8] Shown are absolute frequency measurements in units of hertz,

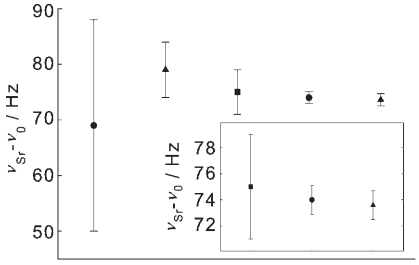

Figure 5. Comparison of recent ^{87}Sr clock frequency (ν_{Sr}) measurements from labs around the world. The fixed offset is $\nu_0 = 429{,}228{,}004{,}229{,}800$ Hz. Circles denote JILA measurements, triangles are Paris measurements, and squares are Tokyo measurements. The inset shows the excellent agreement of the latest results at the hertz level.

obtained by taking the ratio of the Sr clock transition frequency to the frequency of a local Cs clock. The hertz-level agreement is a testament to the reliability of the neutral Sr optical lattice clocks, and a confirmation that systematic shifts are understood at this level. The main systematic effects for the lattice clock can be divided into two categories: those arising from the atomic system, and those from the frequency comparison. The former include ac Stark shifts from the lattice and probe optical fields, and black body radiation from the vacuum chamber walls as well as shifts arising from magnetic fields and atomic collisions in the lattice. The latter include any uncertainties on the Cs clock used for comparison, any errors introduced by frequency transfer between the two clocks, and general relativity effects that arise from different altitudes of the clock locations. The uncertainties in Figure 5 are dominated by frequency counting, and the next generation of comparisons against other optical clocks is expected to reduce the counting uncertainties by more than an order of magnitude. We have measured instabilities of our Sr clock against both the hydrogen maser calibrated to the Cs time standard,[13] and the NIST Ca optical clock.[10] While the Sr-maser instability is $\sim2\times10^{-13}\,\tau^{-1/2}$, where τ is the averaging time in seconds, the optical-optical instability is $<5\times10^{-15}\,\tau^{-1/2}$. An optical–optical comparison would thus greatly reduce the averaging time needed to access the same level of precision. In terms of systematic uncertainties arising from the Sr lattice clock itself, the near-term goal is to reach the limit set by black body radiation effects.[28,31] In the future, this limit can be overcome by improving the knowledge of the clock state polarizabilities near the black body peak, and re-engineering the trapping system for better temperature control.

Ultranarrow Spectral Widths

Typical operation of our optical Sr clock relies on probe-time-limited linewidths of ~10 Hz. Furthermore, the combination of the probe light with a temporal coherence of ~1 s, and the zero-differential-Stark-shift optical lattice trap in which a superposition of the atomic clock states ($^1S_0$ and $^3P_0$) remains intact for at least several seconds, is a starting point for attempting spectroscopy in the optical frequency domain that is coherent on the 1 s time scale.

We have demonstrated hertz-level spectra with Rabi and Ramsey spectroscopy schemes. In both cases, we apply a small magnetic field (~1 gauss) that breaks the degeneracy between π-transitions originating from neighboring sublevels of the ground state arising from the nuclear spin[20] by about 100 Hz. The probe frequency is stepped by about 0.4 Hz and 1 Hz for the Rabi and Ramsey methods, respectively, as the resonance for a single nuclear spin projection is traversed. The Rabi approach[32,33] involves a single long probe pulse to move the atoms from the ground to the metastable state, with the transferred population resonantly dependent on probe laser frequency. The Ramsey approach[32,34] consists of two short pulses that determine the Rabi envelope of the lineshape and are separated by a long free evolution time. The free evolution time sets the width of the fringes within the envelope, and thus the spectral resolution. The fringes arise from interference of two temporal excitation paths (absorbing a photon from the first or the second short pulse).

Both Rabi and Ramsey methods have yielded spectra that are Fourier-limited by the probe pulse duration to about 1.8 Hz. This corresponds to an experimental quality factor of $Q\cong2.4\times10^{14}$, similar to but exceeding the best result to date, achieved with a single mercury ion.[35] One of the main strengths of the neutral atom system is the large number of atoms contributing to the coherent signal. The spectra shown in Figure 6 are therefore obtained with a single scan without averaging or normalization. As described below, setting longer probing or free evolution times resulted in no further improvement in Q.

Ramsey spectroscopy is a useful tool in diagnosing the limitation to the coherence time in the lattice clock. If the system is limited by the lifetime of the atoms in the trap, the Ramsey technique can yield higher fringe resolution at the expense of signal contrast. Even for the same total probe time, the Fourier-limited Ramsey fringe resolution is slightly higher (by about a factor of 2). Since no improvement in resolution was achieved with the Ramsey method, we conclude that the coherence of the spectroscopy was limited by nonlinear frequency noise on the probe laser. In fact, it is more challenging to maintain a good signal to noise ratio during Ramsey spectros-

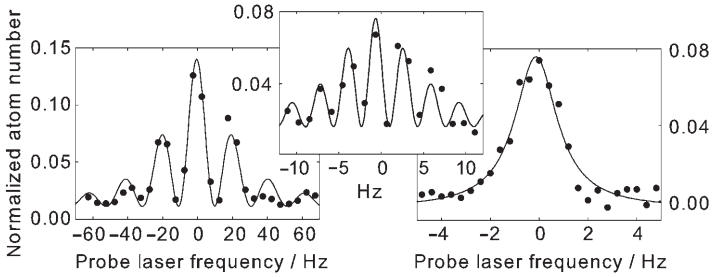

Figure 6. Spectra of the clock transition, with the Zeeman degeneracy removed. The Ramsey spectrum on the left has a 10 Hz wide central feature, and the Rabi spectrum on the right is 2 Hz wide, in agreement with what is expected for the given probing and free evolution times. The inset shows a Ramsey spectrum collected with a longer free evolution time, and the central feature is 1.7 Hz wide.

copy, as it takes at least 20 s to scan across the width of the envelope, which places more stringent constraints on thermal noise of the high finesse laser cavity.

The pursuit of the most stable and accurate time standards require development of more aggressive laser stabilization schemes in order to continue improving the spectroscopic resolution and probe physical effects that contribute to line shifts at an increasingly smaller scale. In the meantime, the achievement of atom-light coherence for nearly a second has already resulted in a precision measurement of the magnetic moment of the $^3P_0$ Sr clock state[20] and a reduction of most systematic clock uncertainties to the 10^{-16}–10^{-17} level.[28] In addition, long atom-light coherence times are invaluable for quantum information and quantum memory research, in which two-electron atoms are expected to play a prominent role.[36]

From Neutral Atoms to Ultracold Molecules

While experimental research on ultracold atoms has seen extensive progress in recent years, ultracold molecules would present unique opportunities for studies of degenerate quantum matter with long-range interactions, for precision measurements, and for understanding the physics of chemical reactions. Creating and trapping ultracold molecules is an active field of research.[37] The most popular approaches start with either high-velocity molecules that must be slowed or cooled[38] or with ultracold atoms that must be bound into molecules.[11,39] The latter approach can take two paths: binding atoms in the ground electronic state by using Feshbach resonances, or employing an optical method of photoassociation that involves an excited electronic state.

Photoassociation (PA) is a process that can be described by $A+A+p \rightarrow A\text{–}A^*$,[11] where A and A^* denote an atom in the ground and excited state, p is a photon near resonance with an excited molecular bound state, and the right-hand side implies a bound state. Significant work has been done on PA with relatively broad transitions (100 s of kHz to 10 s of MHz).[40–43] This has led to accurate measurements of ground state scattering lengths[40,41] that determine the properties of the gas in the ultracold collision regime of *s*-wave scattering.[44]

Our system combines ultracold Sr and narrow linewidth lasers which puts us in a unique position to carry out PA on narrow, forbidden transitions. To take advantage of high isotopic abundance (83%) and absence of nuclear spin, we have chosen to work with ^{88}Sr. PA was performed on the $^1S_0$–$^3P_1$ forbidden transition, with a molecular natural linewidth of about 15 kHz (twice the atomic linewidth). Narrow line PA has several interesting features. One of them is high resolution, which makes the spectroscopy sensitive to the ultracold thermal distribution of the atom cloud and to the dimensional effects of the lattice trap; it also allows to resolve the dense series of bound states near dissociation. Another potential feature is large Franck-Condon (FC) overlaps between bound state wavefunctions in the excited and ground electronic states. For short-lived excited states, the excited-ground state interaction is predominantly resonant dipole-dipole, and decreases as C_3/R^3 with increasing interatomic separation R. For longer-lived metastable states, C_3 is small, and the interatomic potential has a strong contribution from the van der Waals C_6/R^6 term. Since the interaction between two ground state atoms is predominantly van der Waals, the ground and metastable molecular potentials have similar shapes, which enhances the FC factors. The large FC factors naturally lead to considerations of efficient production of bound molecules in the ground electronic state, and of future experiments that can be carried out using the ultracold molecular ensemble.

Narrow Line Photoassociation in an Optical Lattice

The zero-differential-Stark-shift optical lattice technique is readily applicable to PA experiments. The magic wavelength for the $^1S_0$–$^3P_1$ transition is near 914 nm.[45] As before, the PA probe laser at 689 nm ($<$100 Hz linewidth) is directed along the strong confinement axis of the lattice. Long coherence times are useful since the PA process based on the weak transition proceeds relatively slowly. After about 300 ms of PA, the remaining unbound atoms are detected. When the probe laser frequency is scanned, the apparent trap losses correspond to PA resonances.[46]

Long-range Sr_2 molecular potentials are illustrated in Figure 7. The ground state has gerade symmetry and its energy is given by the potential V_g. The excited state ungerade potentials that support transitions to the ground state are 0_u and 1_u (corresponding to the total atomic angular momentum projections onto the internuclear axis of 0 and 1), the latter with a small repulsive barrier. All relevant vibrational states are separated by more than a linewidth, permitting high-resolution spectroscopy. The observed linewidth of the PA resonances is dictated by the thermal distribution of the initial atom cloud (Figure 7). In our case, the 2 μK starting temperature limits the widths to about 100 kHz. A close-up of a typical trap loss resonance is shown in Figure 8. Since the natural linewidth is much smaller than the thermal width, the resonance exhibits the characteristic Maxwell–Boltzmann asymmetry (inset in Figure 8) that increases with initial temperature. For broad-line PA, this asymmetry becomes apparent only at much hotter, millikelvin-

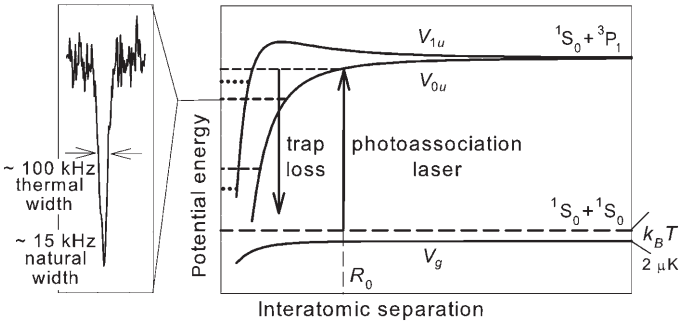

Figure 7. Long-range interatomic potentials of Sr_2, corresponding to the ground state (V_g) and the first excited state with the $^1S_0$–$^3P_1$ dissociation limit (V_{0u} and V_{1u}). On the left is an example of trap loss observed when the photoassociation laser is resonant with a transition from two free atoms to an excited bound state. Although the natural width of the resonance is expected to be about 15 kHz, the observed width of 100 kHz is limited by the 2 μK initial temperature.

level temperatures. In addition, our system is sensitive to the dimensional effects of collisions in the planar lattice sites. The zero-point energy of the trap contributes a significant line shift that requires a correction.

Nine least-bound vibrational levels of the long-range 0_u and 1_u excited molecular potentials were measured and identified (Figure 9). The values of the C_3 and C_6 coefficients were adjusted in the multichannel theoretical model[47] to ensure bound states at the experimentally determined resonance energies. The C_3 coefficient can be expressed in terms of the atomic lifetime τ as $C_3 = 3\hbar c^3/(4\tau\omega^3)$, where $\hbar\omega$ is the atomic transition energy and c is the speed of light. The combination of our experiment and theory yields a C_3 coefficient that corresponds to the $^3P_1$ atomic lifetime of 21.5(2) μs.

Two-electron atoms have no hyperfine splitting in the ground state, and therefore lack magnetic Feshbach resonances. At the same time, the ground state scattering length a of ^{88}Sr is very small[40] and not conducive to evaporative cooling toward quantum degeneracy. However, narrow line PA spectroscopy points toward the possibility of using optical Feshbach resonances[48–50] to enhance the scattering length. In the dressed molecular state picture, the PA photon makes an excited bound state quasi-resonant with the initial scattering state, thus contributing an additional scattering pathway and changing the background scattering length from a to $a + a_{opt}$. In particular, the least-bound state near the $^1S_0$–$^3P_1$ dissociation limit that we observed at the detuning of about -0.4 MHz has a very strong coupling to the initial scattering state (about 10^5 times stronger than the molecular states resolvable with broad line PA). The large strength of this PA transition suggests that it should be possible to use far-detuned PA light for the optical Feshbach resonance, thus avoiding the high trap loss intrinsically associated with PA. It should be noted that previously, the least-bound molecular states

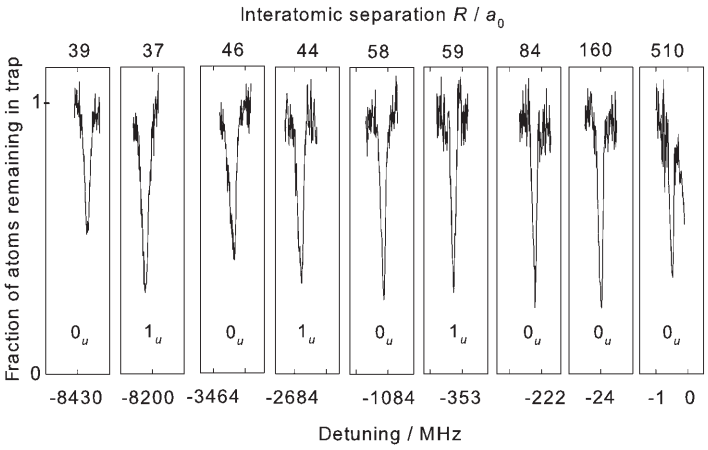

Figure 9. Least-bound vibrational levels of Sr_2 near the $^1S_0$–$^3P_1$ dissociation limit, corresponding to the 0_u and 1_u potentials. While the typical size of the photoassociated molecule is $\sim 100\,a_0$, the last bound state corresponds to a very large dimer with internuclear separation $> 500\,a_0$. Its sloping background is a result of the nearby atomic transition.

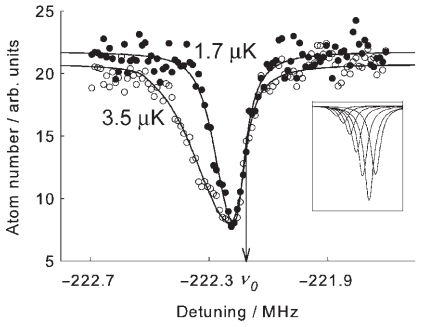

Figure 8. Trap loss resonance corresponding to a bound state of 0_u about 222 MHz below the dissociation limit (the third bound state overall). Even at microkelvin temperatures, thermal effects dominate the narrow spectrum, as can be seen by the broadening when the initial temperature is doubled. The inset illustrates the photoassociation lineshape as a convolution of a Lorentzian transition probability with a Maxwell–Boltzmann thermal distribution. Note that as a result of the line asymmetry, the location of the bound state, denoted by the arrow, is not given by the apparent peak.

have remained elusive because of the proximity of the broad atomic transition. The narrow line PA permits resolution of the least-bound level, which inherently has the strongest coupling to the atomic scattering state.

We estimate that by employing an optical Feshbach resonance based on the least-bound $^1S_0$–$^3P_1$ 0_u molecular level, we should be able to tune a by $a_{opt} \cong \pm 300\,a_0$, where a_0 is the Bohr radius, if the PA laser has an intensity of 10 W cm^{-2} and is far-detuned by $\delta = \pm 160$ MHz from the PA resonance. In contrast, optical tuning of the scattering length in ^{87}Rb Bose–Einstein condensate[49] achieved a tuning range of $a_{opt} \cong \pm 90\,a_0$ at much larger PA laser intensities of 500 W cm^{-2}. In addition, the Sr system at the given parameter values is estimated to have a trap loss rate[48] of only $\sim 2\times10^{-14}$ cm^3 s^{-1} while the loss rate in the ^{87}Rb experiment was 2×10^{-10} cm^3 s^{-1} These values of a_{opt} and atom loss rate for ^{88}Sr would result in elastic and inelastic collision rates of $\Gamma_{el} \cong 600$ s^{-1} and $\Gamma_{inel} \cong 0.1$ s^{-1}. The favorable $\Gamma_{el}/\Gamma_{inel}$ ratio may enable evaporative cooling. However, a possible limitation on the use of optical Feshbach resonances

based on least-bound states is the proximity of the atomic transition (scattering rate of $\Gamma_s \cong \Gamma_{el}/15$ in this example), as excessive one-atom photon scattering can cause heating and trap loss.

Besides efficient optical Feshbach resonances, narrow line PA spectroscopy in an optical lattice opens many research possibilities that include many-atom entanglement for quantum computation[36] and studies of ultracold collisions in 2D and 1D regimes.[51] Another potential application of narrow line PA is efficient production of ultracold molecules in the ground electronic state. For example, bound-bound FC factor calculations show that about 90% of the molecules photoassociated into the -8.4 GHz $^1S_0$–$^3P_1$ 0_u bound state decay to a single ground state vibrational level (distributed between only two rotational sublevels).[52] It appears to be possible to use relatively low power lasers in a two-photon Raman configuration to coherently transfer the vibrationally excited molecules into deeply bound vibrational levels of the electronic ground state.[52] Sr could also be combined with other two-electron atoms such as Yb to create strongly interacting ultracold polar molecules in an optical lattice. Finally, ultracold non-polar Sr_2 molecules in the lattice can serve as a basic system for precision measurements of the drift of fundamental physical constants.

Precision Measurements of Fundamental Constants

Atomic clocks have for a long time provided stringent constraints on drifts of the fine structure constant α and the proton-electron mass ratio, $m_p/m_e \equiv \mu$.[53,54] A molecular clock, or precise measurement of vibrational energy spacings in the electronic ground state of a dimer, would complement the existing atomic clocks in the quest for constraints on time variation of fundamental constants. Particularly, the variation of μ is well suited for measurements with homonuclear molecular species.

While the interatomic potential energy depends on electronic interactions and thus on m_e, the kinetic energy of the atoms is determined by the heavier nuclear mass m_p. The vibrational energy spacings therefore depend only on the ratio μ. Currently, the best laboratory constraints on time variation of μ, below the level of 10^{-14}, are obtained from hyperfine atomic clocks.[54] Unfortunately, hyperfine atomic transitions depend on other fundamental parameters such as the fine structure constant, and separation of the dependences requires theoretical modeling.[53] Recently, cosmological tests of μ variation were carried out on ammonia spectra[55] and hydrogen spectra.[56] The results disagree at the 10^{-15} level. It is critical to perform the test in an independent system, especially one in which any variation arises only because of μ, at least to leading order.

Ultracold molecules in an optical lattice present an ideal, maximally controlled environment for this measurement. We have explored the potential of precision measurements with ultracold Sr_2 molecules in the ground electronic state. While this requires extensive experimental work involving Raman spectroscopy of vibrational levels in the ground and excited electronic states, our simple estimates indicate no fundamental limit to achieving such an ensemble of molecules.[52]

We have analyzed potential systematic effects, and concluded that the initial measurement should be possible at the 10^{-15} level of uncertainty, with a potential to reduce the uncertainty further.[52] Most importantly, the molecular system does not require removal of the effects of fundamental constants other than μ. The systematic effects can be well controlled at the laboratory level, as attested to by the precision of the atomic lattice clock. We can find specific frequencies for the optical lattice, near the global magic wavelength, that cancel ac Stark shifts for the two probed molecular vibrational levels. In other words, there exist zero-differential-Stark-shift lattices for a molecular clock. We have shown that the maximum sensitivity to variation of μ is achieved by measuring the frequency gap between one of the anchor levels near the top or bottom of the molecular potential and a middle vibrational level that has the highest sensitivity to a change in the mass ratio.

Undoubtedly, it takes substantial experimental effort to realize a molecular clock measurement at ultracold temperatures. Nonetheless, it is one of many exciting goals to look forward to, and to keep in mind while building the toolkit required for manipulating molecules at the coldest temperatures and high densities.

Conclusions

Within the last three years, the progress of optical lattice clocks has been very rapid. The systematic uncertainty of the ^{87}Sr clock transition is close to breaking into the 10^{-17} decade, and coherent spectroscopy has been demonstrated with line quality factors above 2×10^{14}. This highly coherent manipulation of large atomic ensembles leads to unprecedented level of timekeeping for fundamental physics such as general relativistic effects and micron scale forces, and for applications such as navigation and geodesy.

Lattice clock techniques have been applied to ultracold molecular physics by photoassociating laser-cooled atoms using a narrow optical transition, an approach that illuminates new physics and suggests methods of obtaining dense samples of ultracold molecules. Multiple quantum information and precision measurement proposals have been put forward that build on our recent results, such as using the nuclear spins of two-electron atoms to switch off electronic interactions through quantum statistics, and utilizing ultracold dimers for model-independent tests of time variation of fundamental constants. It may be only a short time before many of these ideas become reality.

Acknowledgements

We thank Z. Barber, S. Diddams, S. Foreman, T. Fortier, J. Hall, L. Hollberg, T. Ido, M. Martin, M. de Miranda, M. Notcutt, C. Oates, T. Parker, and J. Stalnaker for help with the frequency transfer, the probe laser, and other experimental aspects of the work. We acknowledge theory collaboration with R. Ciuryło, P. Julienne, S.

Kotochigova, and P. Naidon. The funding was provided by NSF, NIST, and ONR.

Keywords: atomic clock · molecular trapping · optical processes · Ramsey spectroscopy · ultracold atoms

[1] W. D. Phillips, *Rev. Mod. Phys.* **1998**, *70*, 721–741; C. E. Wieman, D. E. Pritchard, D. J. Wineland, *Rev. Mod. Phys.* **1999**, *71*, S253–S262.
[2] E. A. Cornell, C. E. Wieman, *Rev. Mod. Phys.* **2002**, *74*, 875–893; W. Ketterle, *Rev. Mod. Phys.* **2002**, *74*, 1131–1151; B. DeMarco, D. S. Jin, *Science* **1999**, *285*, 1703–1706.
[3] J. J. García-Ripoll, P. Zoller, J. I. Cirac, *J. Phys. B* **2005**, *38*, S567–S578.
[4] A. Peters, K. Y. Chung, S. Chu, *Nature* **1999**, *400*, 849–852; P. Cladé, E. de Mirandes, M. Cadoret, S. Guellati-Khélifa, C. Schwob, F. Nez, L. Julien, F. Biraben, *Phys. Rev. Lett.* **2006**, *96*, 033 001.
[5] S. A. Diddams, J. C. Bergquist, S. R. Jefferts, C. W. Oates, *Science* **2004**, *306*, 1318–1324.
[6] M. M. Boyd, A. D. Ludlow, S. Blatt, S. M. Foreman, T. Ido, T. Zelevinsky, J. Ye, *Phys. Rev. Lett.* **2007**, *98*, 083002.
[7] R. Le Targat, X. Baillard, M. Fouche, A. Brusch, O. Tscherbakoff, G. D. Rovera, P. Lemonde, *Phys. Rev. Lett.* **2006**, *97*, 130801.
[8] M. Takamoto, F.-L. Hong, R. Higashi, Y. Fuji, M. Imae, H. Katori, *J. Phys. Soc. Jpn.* **2006**, *75*, 104302.
[9] Z. W. Barber, C. W. Hoyt, C. W. Oates, L. Hollberg, A. V. Taichenachev, V. I. Yudin, *Phys. Rev. Lett.* **2006**, *96*, 083002.
[10] G. Wilpers, C. W. Oates, L. Hollberg, *Appl. Phys. B* **2006**, *85*, 31–44.
[11] K. M. Jones, E. Tiesinga, P. D. Lett, P. S. Julienne, *Rev. Mod. Phys.* **2006**, *78*, 483–535.
[12] T. Köhler, K. Góral, P. S. Julienne, *Rev. Mod. Phys.* **2006**, *78*, 1311–1361.
[13] T. P. Heavner, S. R. Jefferts, E. A. Donley, J. H. Shirley, T. E. Parker, *Metrologia* **2005**, *42*, 411–422.
[14] F. Ruschewitz, J. L. Peng, H. Hinderthur, N. Schaffrath, K. Sengstock, W. Ertmer, *Phys. Rev. Lett.* **1998**, *80*, 3173–3176; E. A. Curtis, C. W. Oates, L. Hollberg, *QELS Technical Digest Series, Vol. 74*, Optical Society of America, Washington DC, **2002**, p. 53; K. R. Vogel, T. P. Dinneen, A. Gallagher, J. L. Hall, *IEEE Trans. Instrum. Meas.* **1999**, *48*, 618–621; T. Mukaiyama, H. Katori, T. Ido, Y. Li, M. Kuwata-Gonokami, *Phys. Rev. Lett.* **2003**, *90*, 113002; H. Hachisu, K. Miyagishi, S. G. Porsev, A. Derevianko, V. D. Ovsiannikov, V. G. Pal'chikov, M. Takamoto, H. Katori, *arXiv:0711.4638*; R. Maruyama, R. H. Wynar, M. V. Romalis, A. Andalkar, M. D. Swallows, C. E. Pearson, E. N. Fortson, *Phys. Rev. A* **2003**, *68*, 011 403(R).
[15] G. Ferrari, N. Poli, F. Sorrentino, G. M. Tino, *Phys. Rev. Lett.* **2006**, *97*, 060402.
[16] H. Katori, M. Takamoto, V. G. Pal'chikov, V. D. Ovsiannikov, *Phys. Rev. Lett.* **2003**, *91*, 173005.
[17] J. Ye, D. W. Vernooy, H. J. Kimble, *Phys. Rev. Lett.* **1999**, *83*, 4987–4990.
[18] R. H. Dicke, *Phys. Rev.* **1953**, *89*, 472–473; D. Leibfried, R. Blatt, C. Monroe, D. Wineland, *Rev. Mod. Phys.* **2003**, *75*, 281–324.
[19] S. G. Porsev, A. Derevianko, *Phys. Rev. A* **2004**, *69*, 042506; R. Santra, K. V. Christ, C. H. Greene, *Phys. Rev. A* **2004**, *69*, 042510.
[20] M. M. Boyd, T. Zelevinsky, A. D. Ludlow, S. Blatt, T. Zanon-Willette, S. M. Foreman, J. Ye, *Phys. Rev. A* **2007**, *76*, 022510.
[21] V. S. Bagnato, A. Aspect, S. C. Zilio, *Opt. Commun.* **1989**, *72*, 76–81.
[22] T. H. Loftus, T. Ido, M. M. Boyd, A. D. Ludlow, J. Ye, *Phys. Rev. A* **2004**, *70*, 063413.
[23] M. W. Fleming, A. Mooradian, *IEEE J. Quantum Electron.* **1981**, *17*, 44–59.
[24] M. Notcutt, L.-S. Ma, J. Ye, J. L. Hall, *Opt. Lett.* **2005**, *30*, 1815–1817; A. D. Ludlow, X. Huang, M. Notcutt, T. Zanon-Willette, S. M. Foreman, M. M. Boyd, S. Blatt, J. Ye, *Opt. Lett.* **2007**, *32*, 641–643.
[25] R. W. P. Drever, J. L. Hall, F. V. Kowalski, J. Hough, G. M. Ford, A. J. Munley, H. Ward, *Appl. Phys. B* **1983**, *31*, 97–105.
[26] K. Numata, A. Kemery, J. Camp, *Phys. Rev. Lett.* **2004**, *93*, 250602.
[27] T. M. Fortier, D. J. Jones, S. T. Cundiff, *Opt. Lett.* **2003**, *28*, 2198–2200; S. T. Cundiff, J. Ye, J. L. Hall, *Rev. Sci. Instrum.* **2001**, *72*, 3749–3771; R. Holzwarth, Th. Udem, T. W. Hänsch, J. C. Knight, W. J. Wadsworth, P. St. J. Russell, *Phys. Rev. Lett.* **2000**, *85*, 2264–2267.
[28] A. D. Ludlow, T. Zelevinsky, G. K. Campbell, S. Blatt, M. N. Boyd, M. H. G. de Miranda, M. J. Martin, J. W. Thomsen, S. M. Foreman, J. Ye, T. M. Fortier, J. E. Stalnaker, S. A. Diddams, Y. te Coq, Z. W. Barber, N. Poli, N. D. Lemke, K. M. Beck, C. W. Oates, unpublished results.
[29] S. M. Foreman, A. D. Ludlow, M. H. G. de Miranda, J. E. Stalnaker, S. A. Diddams, J. Ye, *Phys. Rev. Lett.* **2007**, *99*, 153601.
[30] A. D. Ludlow, M. M. Boyd, T. Zelevinsky, S. M. Foreman, S. Blatt, M. Notcutt, T. Ido, J. Ye, *Phys. Rev. Lett.* **2006**, *96*, 033003.
[31] S. G. Porsev, A. Derevianko, *Phys. Rev. A* **2006**, *74*, 020502.
[32] M. M. Boyd, T. Zelevinsky, A. D. Ludlow, S. M. Foreman, S. Blatt, T. Ido, J. Ye, *Science* **2006**, *314*, 1430–1433.
[33] I. I. Rabi, S. Millman, P. Kusch, J. R. Zacharias, *Phys. Rev.* **1939**, *55*, 526–535.
[34] N. F. Ramsey, *Metrologia* **2005**, *42*, S1–S3.
[35] R. J. Rafac, B. C. Young, J. A. Beall, W. M. Itano, D. J. Wineland, J. C. Bergquist, *Phys. Rev. Lett.* **2000**, *85*, 2462–2465.
[36] D. Hayes, P. S. Julienne, I. H. Deutsch, *Phys. Rev. Lett.* **2007**, *98*, 070501; I. Reichenbach, I. H. Deutsch, *Phys. Rev. Lett.* **2007**, *99*, 123001.
[37] J. Doyle, B. Friedrich, R. V. Krems, F. Masnou-Seeuws, *Eur. Phys. J. D* **2004**, *31*, 149–164.
[38] R. deCarvalho, J. M. Doyle, B. Friedrich, T. Guillet, J. Kim, D. Patterson, J. D. Weinstein, *Eur. Phys. J. D* **1999**, *7*, 289–309; H. L. Bethlem, G. Meijer, *Int. Rev. Phys. Chem.* **2003**, *22*, 73–128; E. R. Hudson, J. R. Bochinski, H. J. Lewandowski, B. C. Sawyer, J. Ye, *Eur. Phys. J. D* **2004**, *31*, 351–358.
[39] J. M. Sage, S. Sainis, T. Bergeman, D. DeMille, *Phys. Rev. Lett.* **2005**, *94*, 203001; F. K. Fatemi, K. M. Jones, P. D. Lett, E. Tiesinga, *Phys. Rev. A* **2002**, *66*, 053401.
[40] P. G. Mickelson, Y. N. Martinez, A. D. Saenz, S. B. Nagel, Y. C. Chen, T. C. Killian, *Phys. Rev. Lett.* **2005**, *95*, 223002; M. Yasuda, T. Kishimoto, M. Takamoto, H. Katori, *Phys. Rev. A* **2006**, *73*, 011 403(R).
[41] K. Enomoto, M. Kitagawa, K. Kasa, S. Tojo, Y. Takahashi, *Phys. Rev. Lett.* **2007**, *98*, 203201.
[42] C. Degenhardt, T. Binnewies, G. Wilpers, U. Sterr, F. Riehle, *Phys. Rev. A* **2003**, *67*, 043408.
[43] C. McKenzie, J. H. Denschlag, H. Häffner, A. Browaeys, L. E. E. de Araujo, F. K. Fatemi, K. M. Jones, J. E. Simsarian, D. Cho, A. Simoni, E. Tiesinga, P. S. Julienne, K. Helmerson, P. D. Lett, S. L. Rolston, W. D. Phillips, *Phys. Rev. Lett.* **2002**, *88*, 120403; C. C. Tsai, R. S. Freeland, J. M. Vogels, H. M. J. M. Boesten, B. J. Verhaar, D. J. Heinzen, *Phys. Rev. Lett.* **1997**, *79*, 1245–1248.
[44] J. Weiner, V. S. Bagnato, S. Zilio, P. S. Julienne, *Rev. Mod. Phys.* **1999**, *71*, 1–85.
[45] T. Ido, H. Katori, *Phys. Rev. Lett.* **2003**, *91*, 053001.
[46] T. Zelevinsky, M. M. Boyd, A. D. Ludlow, T. Ido, J. Ye, R. Ciuryło, P. Naidon, P. S. Julienne, *Phys. Rev. Lett.* **2006**, *96*, 203201.
[47] R. Ciuryło, E. Tiesinga, S. Kotochigova, P. S. Julienne, *Phys. Rev. A* **2004**, *70*, 062 710.
[48] R. Ciuryło, E. Tiesinga, P. S. Julienne, *Phys. Rev. A* **2005**, *71*, 030 701(R).
[49] M. Theis, G. Thalhammer, K. Winkler, M. Hellwig, G. Ruff, R. Grimm, J. H. Denschlag, *Phys. Rev. Lett.* **2004**, *93*, 123001.
[50] F. K. Fatemi, K. M. Jones, P. D. Lett, *Phys. Rev. Lett.* **2000**, *85*, 4462–4465.
[51] P. Naidon, P. S. Julienne, *Phys. Rev. A* **2006**, *74*, 062713.
[52] S. Kotochigova, *J. Chem. Phys.* **2008**, *128*, 024303; T. Zelevinsky, S. Kotochigova, J. Ye, *Phys. Rev. Lett.* **2008**, *100*, 043201.
[53] T. M. Fortier, N. Ashby, J. C. Bergquist, M. J. Delaney, S. A. Diddams, T. P. Heavner, L. Hollberg, W. M. Itano, S. R. Jefferts, K. Kim, F. Levi, L. Lorini, W. H. Oskay, T. E. Parker, J. Shirley, J. E. Stalnaker, *Phys. Rev. Lett.* **2007**, *98*, 070801; M. Zimmermann, M. Fischer, N. Kolachevsky, R. Holzwarth, T. Udem, T. W. Hänsch, M. Abgrall, J. Griinert, I. Maksimovic, S. Bize, H. Marion, F. P. Dos Santos, P. Lemonde, G. Santarelli, P. Laurent, A. Clairon, C. Salomon, *Laser Phys.* **2005**, *15*, 997–1009.
[54] S. G. Karshenboim, V. Flambaum, E. Peik, *arXiv:0410074*.
[55] V. V. Flambaum, M. G. Kozlov, *Phys. Rev. Lett.* **2007**, *98*, 240801.
[56] E. Reinhold, R. Buning, U. Hollenstein, A. Ivanchik, P. Petitjean, W. Ubachs, *Phys. Rev. Lett.* **2006**, *96*, 151101.

Received: October 25, 2007

